Experimental investigation of bypassed-oil recovery in tight reservoir rock using a two-step CO2 soaking strategy: Effects of fracture geometry

Article · July 2023

CITATIONS
0

READS
23

7 authors, including:

Muhend Milad
7 PUBLICATIONS **59** CITATIONS
SEE PROFILE

Radzuan Junin
Universiti Teknologi Malaysia
195 PUBLICATIONS **4,301** CITATIONS
SEE PROFILE

Akhmal Sidek
Universiti Teknologi Malaysia
62 PUBLICATIONS **272** CITATIONS
SEE PROFILE

Abdulmohsin Imqam
Missouri University of Science and Technology
101 PUBLICATIONS **1,541** CITATIONS
SEE PROFILE

Upstream Oil and Gas Technology 11 (2023) 100093

Contents lists available at ScienceDirect

Upstream Oil and Gas Technology

journal homepage: www.sciencedirect.com/journal/upstream-oil-and-gas-technology

Experimental investigation of bypassed-oil recovery in tight reservoir rock using a two-step CO_2 soaking strategy: Effects of fracture geometry

Muhend Milad [a,b,f,*], Radzuan Junin [a,c], Akhmal Sidek [a,c], Abdulmohsin Imqam [d], Gamal A. Alusta [e], Agi Augustine [a], Muhanad A. Abdulazeez [a]

[a] Department of Petroleum Engineering, School of Chemical and Energy Engineering, Faculty of Engineering, Universiti Teknologi Malaysia, Johor Bahru 81310, Malaysia
[b] Department of Petroleum Engineering, School of Oil and Gas Engineering, Faculty of Engineering, University of ZAWIA, Libya
[c] Institute for Oil and Gas (IFOG), Universiti Teknologi Malaysia, Johor Bahru 81310, Malaysia
[d] Department of Geosciences and Geological and Petroleum Engineering, School of Petroleum Engineering, Missouri University of Science and Technology, Rolla, MO, USA.
[e] Oil & Gas Administrator Instructor, CDI College, Alberta, Canada
[f] Department of Petroleum Engineering, Faculty of Engineering, Al-Rifaq University, Tripoli, Libya

ARTICLE INFO

Keywords:
Tight rock oil recovery
Huff-n-puff
Fracture geometry
Two-step Co2 soaking method
Fracture surface area

ABSTRACT

The potential of the CO_2 soaking procedure has been generally acknowledged as a valid way to advance the tight rock oil recovery. Over the last decade, a significant number of Huff-n-Puff (H-n-P) experiments have been conducted to develop unconventional oil reservoirs. However, the majority of experiments used fully saturated cores and unconfined core holders. Therefore, the average oil recovery at the field-scale could not be accurately estimated. Besides, the effect of key factors such as fracture geometry on bypassed oil recovery has remained obscure. For better quantifying CO_2 H-n-P efficiency in oil fields, this study proposes an immiscible CO_2 soaking process aimed at bypassing the oil before conducting the H-n-P process using various fracture forms and dimensions. Tight cores from Sarawak with an average porosity and permeability of 9% and 0.07 md, respectively, were employed in this experimental research. The importance of the fracture surface areas (FSA), fracture depth (FD), width (FW), and diameter was thoroughly studied. The research findings revealed that the two-step CO_2 soaking procedure significantly reduces the effectiveness of the currently applied laboratory H-n-P process. However, the outcomes are more consistent with the current average oil recoveries in field pilots. The study demonstrates that FD is the most critical factor in maximizing the remaining oil recovery. The research indicates that the FSA does not always follow a specific trend. It is, however, dependent on the fracture geometry. The significance of the crack's surface area and fracture intensity is determined to be primarily dependent on the fracture shape and the utilized core holder system, respectively. The study's findings presented a higher degree of accuracy in estimating actual oil recovery from tight reservoirs employing two-step soaking technology.

1. Introduction

The advancement in hydraulic fracturing in horizontal wells has made it possible for several countries to produce unconventional oil [60]. Unconventional formations such as the Bakken, Permian Basin, and Eagle Ford have made an undeniable contribution to shale oil production and transformed the energy landscape in several states in the United States [5,13,28,36]. However, with the existing technologies, only less than 10% can be retrieved through primary depletion [39,55]. According to Clark [18], the most likely value for the oil recovery factor (RF) in shale oil reservoirs is approximately 7%. After an unconventional well is fractured, oil production typically drops to less than 20% of the

Abbreviations: H-n-P, huff-n-puff; EOR, enhanced oil recovery; FSA, fracture surface areas; FD, fracture depth; FW, fracture width; RF, recovery factor; Soi, initial oil saturation; Sor, residual oil saturation; MMP, minimum miscibility pressure; MCM, multi-contact miscibility; BPR, back-pressure regulator; CL, core length; CD, core diameter; CV, core volume; CSA, core surface area; CLA, core lateral area; FL, fracture length; FV, fracture volume; UTM, Universiti Teknologi Malaysia; W_{dry}, weight of dry core.

* Corresponding author at: Department of Petroleum Engineering, School of Chemical and Energy Engineering, Faculty of Engineering, Universiti Teknologi Malaysia, Johor Bahru 81310, Malaysia.
E-mail address: m.milad@zu.edu.ly (M. Milad).

https://doi.org/10.1016/j.upstre.2023.100093
Received 30 May 2022; Received in revised form 21 May 2023; Accepted 10 July 2023
Available online 20 July 2023

initial rate within one year [14,39]. Thus, tight formations have been identified as limited natural energy reservoirs due to their poor physical properties and sharp decline rate in primary production. The lack of possibilities for extending the life span of numerous shale/tight oil wells leaves companies with no options, forcing them to drill additional wells to maintain the production rate. However, drilling is costly and carries environmental challenges [32]. One major issue with new wells is the re-fracking job because new wells need to be re-fracked frequently due to the limited drainage radius. Therefore, innovative technologies are required to extract the remaining oil from matured reservoirs to maintain profitable oil production volumes [8,9,16]. Scholars have persistently worked on developing of new procedures to increase the recovery factor in tight oil reservoirs. Unfortunately, they found that techniques that have been successfully implemented in conventional reservoirs are not economically efficient, which does not warrant any further technological research [58].

To improve unconventional oil recovery, research on the Huff-n-Puff technique of (H-*n*- P) has been reported. This process is widely employed in North America and China [17] and is found to be cost-effective and more efficient in low-permeability formations [45]. This method has also been successfully employed in high viscous reservoirs for decades [31,34]. Over the last few years, a great amount of bypassed oil in unconventional reservoirs have further aroused wide concern about the application of the H-n-P development. Several laboratory gas H-n-P studies have been performed to access greater quantities of the remaining oil, and in this instance, a wide variety of parameters and methodologies have been considered [3,7,15,23,24,26,46,54,56,74]. Most researchers approved the method of the H-n-P system; however, they disagreed over the role of some critical mechanisms and key parameters due to the lack of actual field data [48]. Other researchers ([6]; Fiallos [25]) claimed that the technique has a considerable performance only when close to the fracture. Despite the success of numerous researchers demonstrating the effectiveness of the H-n-P technique in producing tight oil, its success in extracting bypassed oil under in-situ reservoir conditions remains indistinct. While pilot studies on natural oil-bearing systems can provide declarative knowledge of the enhanced oil recovery (EOR) method's efficiency, comparative studies may not be feasible. Another drawback of pilot projects is their cost of over several million dollars. While laboratory tests can be performed at considerably lower costs [10,37,46]. On the other hand, there are substantial discrepancies between laboratory-generated EOR efficiencies and those discovered through field observations [48]. Generally speaking, several H-n-P laboratory studies reported substantial oil recoveries of up to 100%, yet, the average oil recoveries in field pilots are only 30% [33, 47].

Recent studies demonstrate attempts to replicate improved oil recovery from matrix-fracture combinations, especially in tight reservoirs. This is accomplished by placing high-permeability spacers on core surfaces to imitate fractures [44]. Other laboratory studies have used pre-saturated cores in high-pressure vessels (B. [38]). Such models are incapable of simulating reservoir conditions where the matrix's surface area is not specified. Artificial fractures are, therefore, essential for evaluating key mechanisms for managing injected gas transport into the matrix. And also critical for assessing operational procedures such as soaking time, number of cycles, injection pressure time, production pressure time, etc.

At present, there is literature on numerous laboratory cases. [1,70, 76], reporting favorable performance of the CO_2 H-n-P method performed on tight oil extraction. However, there are limited experimental studies with an emphasis on fracture geometry. Despite the fact that the presence of the fracture network increases the gas-swept area, enlarges the oil flow path, and contributes to the enhancement of oil recovery, it also presents some difficulties. For instance, several studies have demonstrated that in the late stages of oil development, the injected gas travels along the cracks and is unable to make contact with the oil in the matrix, resulting in minimal oil recovery [69]. Furthermore, a valuable study was conducted by Niu and Schechter [50] to understand the influence of fracture geometry on H-n-P performance. Nevertheless, further knowledge is required regarding the significance of FSA for bypassed oil recovery in a more realistic reservoir condition. Subsequently, many research findings have been reviewed to explore the fracture's potential in H-n-P [29,46,50,62]. Unfortunately, the majority of the studies focused on the overall success of the operating factors and conditions. However, the existing literature does not emphasise on the conclusions regarding the surface area of different fractures [48].

Based on the authors' knowledge, no studies have underlined the significance of FSA using various fracture models for validating the H-n-P performance and key factors such as fracture width (FW), fracture depth (FD), and fracture diameter.

Even though CO_2 H-n-P technology has been thoroughly researched [29,41,63,70], most of the previous experimental findings have validated the H-n-P procedure using fully oil-saturated cores. This suggests that the oil removed did not accurately represent the depleted horizontal wells. All of the aforementioned limitations increase the uncertainty surrounding earlier gas cyclic results, indicating that only a few experiments have quantified the H-n-P system's efficiency under realistic reservoir conditions.

In this research, an advanced two-step soaking method was developed to quantify the efficiency of CO_2 H-n-P in depleted tight formations. An immiscible CO_2 soaking method was employed ahead of the H-n-P procedures to bypass the oil as required using un-fractured and fractured cores. This method is utilized to change the core saturation from the initial oil saturation (Soi) to residual oil saturation (Sor), allowing for better investigation of primary depleted wells. This suggests that the H-n-P procedure that follows would be implemented to estimate the recovery of bypassed oil. This research adds new insight and opens new frontiers on evaluating the performance of the H-n-P technique in the actual oil field. Consequently, reducing the current gap between experimental conclusions and field results. More importantly, this research provides a detailed perspective and ground-breaking conclusions regarding the main H-n-P processes and identifies the fracture property that is more significant for improving the hydraulic fracture design. Generally, the two-step CO_2 soaking strategies were developed based on the following considerations: (1) the soaking system helps the molecular diffusion mechanisms to attain a maturity level [21]; (2) the extended soaking process can better validate the application of the H-n-P method, especially in tight/shale fields [48]; (3) the severe need for modified methods capable of replicating reservoir conditions that closely simulate EOR in fracked tight oil formations [46]; (4) the soaking process contributes to the replication of the reservoir's original fluid distribution by transporting crude oil into the matrix via fractures [64]; (5) the CO_2 soaking process likely leads the in-situ system to be more water-wet [53]; (6) the molecular diffusion is the dominant mechanism of CO_2 distribution in the reservoir during the soaking process [56]; (7) similar processes have been demonstrated to be successful approaches to extracting non-bypassed oil systems [43]; and (8) similar processes have been demonstrated to be successful approaches to extracting bypassed oil systems [21]. However, its effectiveness as a means of extracting the remaining tight oil, and the elements affecting its efficiency (e.g., fracture geometry), are still ambiguous given the scarce number of articles on the subject.

2. Experimental

Recently, the H-n-P methodology has been an efficacious EOR procedure applied to numerous tight reservoirs [3,9,22,30,40,66,68,70,76] and shale formations [20,24,46,51,57,61,62,73,74,76]. In this research, similar tools are employed to design gas injection systems. However, improved procedures are also applied and proven better to evaluate the technique. Two CO_2 soaking methods were applied in this study. The first is the CO_2 immiscible soaking process, which is conducted to bypass the oil as required. The second approach is a miscible CO_2 soaking

procedure that was carried out to extract the remaining oil in the matrix. The two-step soaking methods are intended to simulate the actual H-n-P process in the oil field.

2.1. Experimental materials

2.1.1. Core samples

The cores utilized to simulate the bypassed oil were tight sandstone, collected from the Sarawak basin in Malaysia. They mainly consisted of quartz (56.81%), orthoclase (03%), albite (09%), calcite (08%), and ankerite (04%). The cores were between 4 and 7.5 cm in length, and an average of 4.9 cm in diameter. Table 1 presents the measured dimensions of the cores and fractures used in this research. The cores were divided into groups based on the objective of the study.

2.1.2. Fluids

Synthetic oil (diesel) was used as a light oil to saturate cores. The measured density and viscosity of the diesel were 0.84 gm/cm^3 and 5.975 mm^2/s, respectively. The API gravity was 42° A commercial carbon dioxide cylinder with a purity level of 99.99% was utilized for gas injection. The minimum miscible pressure (MMP) of the CO_2/oil was 1253 psi based on 20 ft slim tube tests (STT). Hence, the injection processes were operated under 800 psi and 1750 psi, representing immiscible and multi-contact miscibility (MCM), respectively.

2.1.3. Experiment tools

A variety of tools were used in this study to build multiple setups, including oil saturation and CO_2 injection sets. The schematic diagrams of the performed experiments are presented and explained in the next section. Two different core holders, with and without a confining pressure system, were employed in this experiment to house the core sample. High-pressure gauges were cautiously positioned in the setup to record the pressure throughout the CO_2 injection time, soaking period, and production stage. Two and three-way valves were securely equipped. High-pressure regulators were employed to pressurize the system. Two back-pressure regulators (BPR) were used to ensure that the desired core pressure is maintained at the required level. The backpressure was applied by using N_2 as the pressurizing medium. Two saturation vessels, along with a vacuum pump, were employed to clean up the system and saturate the core samples. To provide a confining pressure to the core holder, a manual pump was employed (maintained at 500 psi above the pressure inside). An air path oven was utilized to achieve the expected reservoir temperature. An accumulator with a 500D syringe pump was employed to store the CO_2 and then injected into the core holder. This combined system was also applied to thrust the oil into the core vessel while maintaining a high saturation pressure at the same time. The syringe pump was mainly used for boosting the pressure and ensuring that the injected fluid pressure reached the predesigned test value. A collector vessel was used to accrue the oil that was produced.

2.2. Experimental setups

This section describes the schematic diagrams of the experimental setup created for core saturation and soaking procedures. The study has three stages: the saturation process, the CO_2 immiscible approach (first soaking step), and the miscible CO_2 H-n-P test (second soaking step). The system shown in Fig. 1 presents the schematic setup for the core saturation experiments operated for the oil saturation process. Details of the experimental setups are reported in Li et al. [39]. The technique used for core saturation consists of two different stages, as shown in Fig. 1. After the cores are dried at 248°F, weighed, while major properties such as porosity and permeability are measured, they are saturated using two different saturation vessels, stages A and B. As soon as the cores were fully saturated and prepared for the EOR test, they were placed in the conventional core holder to perform the first soaking step. The schematic setup is modified to bypass the oil as required (Fig. 2). A similar system has already been developed and reported by several researchers [2,6,12]. After the immiscible soaking process is completed, CO_2 H-n-P attempts are carried out to recover the remaining oil using two different investigation systems. Figs 3 and 4 represent the schematic design assembled to perform H-n-P operations using both the confined and free path systems.

It can be noticed from Fig. 2 that two injection ends (valve-1 and valve-2), as well as a production end (valve-5), are present. During the first-step soaking, immiscible CO_2 injection procedure, valve-2 is locked, and the CO_2 is injected using valve-1. When the CO_2 is injected into the fracture, it becomes in direct contact with the intended sides of the matrix (in contrast to the free path design). Therefore, the CO_2 moves along the constructed space to bypass the oil (as expected). Both BPRs are accurately controlled during the injection practice to ensure that the pressure inside the core holder is continued at the required level. Then, a confining pressure pump is applied to restrain the core inside the rubber sleeve and ensure that the CO_2 will not make any contact with the core sides, except through the designed fractures. After soaking, the gas, together with the oil, is produced by releasing the back pressure through BPR-1. Due to the core being placed vertically inside the conventional core holder, an additional gravity force is achieved to easily produce the oil and guarantee that the extracted fluid will not be infused into the core sample. These soaking procedures are continued until no substantial change is observed or the extracted oil is exhausted.

The immiscible process is carried out in anticipation of simulating the displacement process of the hydraulic fracture technology in an actual horizontal well. Evidently, in a real shale oil reservoir, 5–10% of the original oil in place is recovered using the hydraulic fracturing

Table 1
The dimensions of cores and fractures.

Sample	Core dimensions					Fracture dimensions				
	CL	CD	CV	CSA	CLA	FL	FD	FW	FV	FSA
1	7.4	4.9	139.54	151.62	113.91	4.9	1.3	0.2	1.274	13.72
2	7.4	4.9	139.54	151.62	113.91	4.9	0.5	0.2	0.490	5.88
3	6.2	4.9	116.91	133.15	95.44	4.9	2.6	0.5	6.370	27.93
4	6.2	4.9	116.91	133.15	95.44	4.9	2	3	29.40	34.30
5	5.5	4.9	103.71	122.38	84.66	4.9	3	0.5	7.35	31.85
6	4	4.9	75.42	99.29	61.57	4	0.1	0.3	0.12	2.00
7	4	4.9	75.42	99.29	61.57	4	0.1	0.3	0.12	4.00
8	6.2	4.9	116.91	133.15	95.44	/	/	/	/	/
9	6.2	4.9	116.91	133.15	95.44		Unknown (in-situ fracture)			
10	6.2	4.9	116.91	133.15	95.44	/	/	/	/	/
11	6.2	4.9	116.91	133.15	95.44	/	/	/	/	/
12	4	4.9	75.42	99.29	61.57	4	0.1	0.3	0.12	2.00
13	4	4.9	75.42	99.29	61.57	4	0.1	0.3	0.12	4.00

Note: Core dimensions: CL (core length, cm); CD (core diameter, cm); CV (core volume, cm^3); CSA (core surface area, cm^2); CLA (core lateral area, cm^2).
Fracture dimensions: FL (fracture length, cm); FD (fracture depth, cm); FW (fracture width, cm); FV (fracture volume, cm^3); FSA (fracture surface area, cm^2).

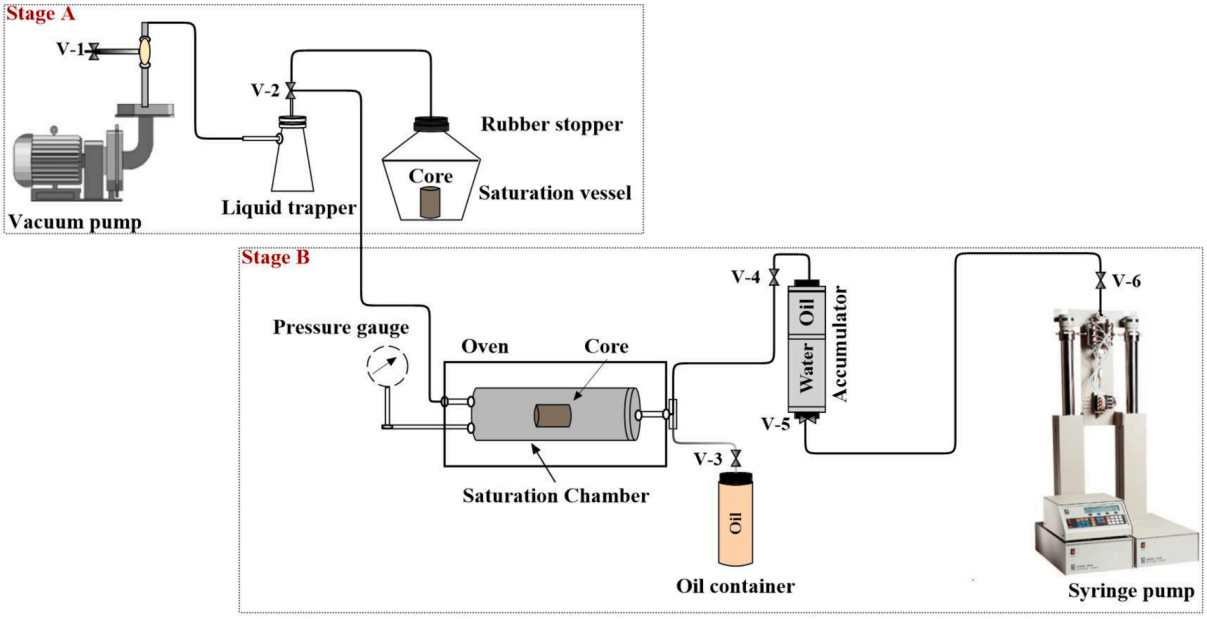

Fig. 1. Schematic of the setup for the core saturation experiments.

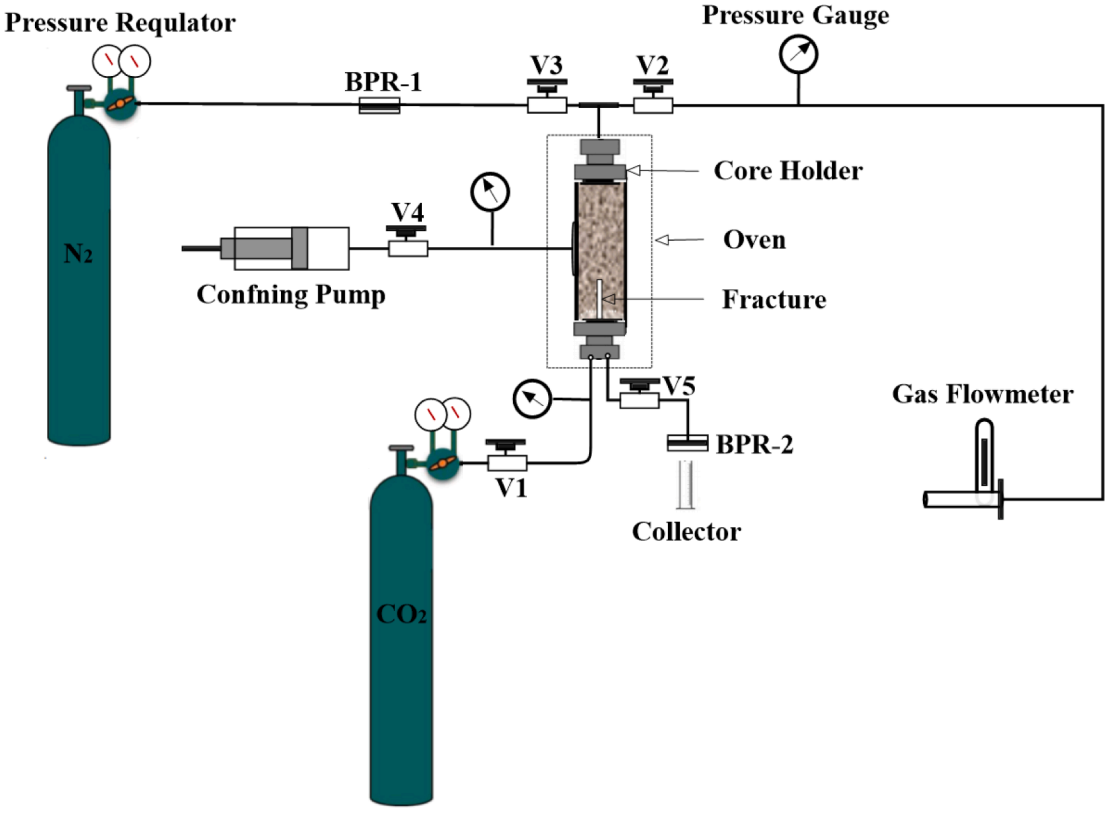

Fig. 2. Experimental schematic diagram of the modified confined system for immiscible soaking test.

knowledge [19]. Thus, nearly 90% of oil is bypassed [73]. This soaking process is done in the hope of simulating the field process by producing a small amount of saturated oil and distributing the remaining oil into the smaller pores of the core [11]. The formed fracture's width, depth, and diameter are adjustable to simulate various fracture areas. After the oil is bypassed using the first immiscible soaking approach, procedures are repeated in a miscible H-n-P mode using the same cores; however, dissimilar systems are employed. Note that both soaking methods, immiscible and miscible, are performed using a similar reservoir temperature. As a result, the soaking time effect can be evaluated more effectively.

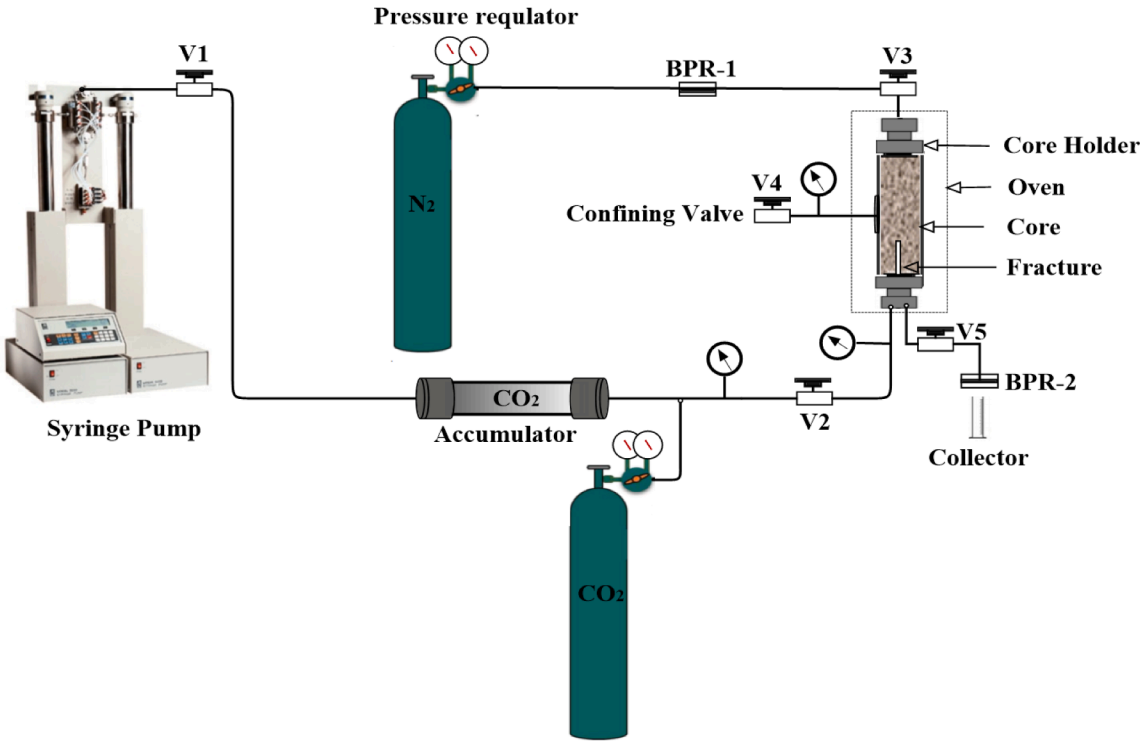

Fig. 3. Experimental schematic diagram of the modified confined system for H-n-P test.

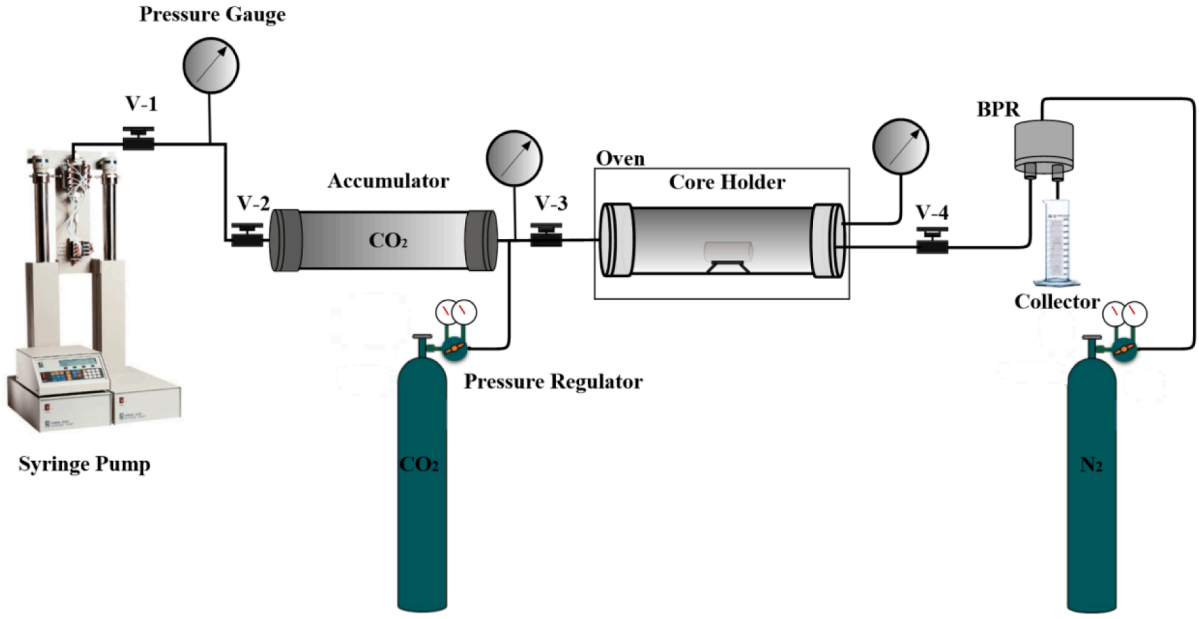

Fig. 4. Schematic of the free path setup for the CO_2 H-n-P experiment.

2.3. Experimental procedures

2.3.1. Core fracture design

The samples used in this study are tight sandstones (Sarawak region, Malaysia) acquired from a geology lab at UTM. Several cylindrical plugs were prepared based on the objectives of the study and each contained a certain orientated artificial (induced) fracture. One category of these fractures was centerline fractures (along the core's diameter), specifically for investigating the FSA, including FW and FD. Another was generated on the outside core surface (along the core's length) to assess the number of formed fractures. The third design was a hole in the core center to further investigate the FSA. The primary central fracture was created by dividing the plug into sides within a certain depth and width. The subsequent one was a straight line with specific dimensions along the core length. The first and second types of fractures were formed using a special grinder and various diameter discs compatible with the core surface type. Regarding the hole fracture that was created in the center, special drill bits for sandstone with various diameters (0.2 cm, 0.3 cm, and 0.5 cm) were used to make the fracture. Performing the above-stated fractures along with the overburden pressure system

enables simulating fractured horizontal wells at a more realistic reservoir condition. Fig. 5 (a, b, and c) shows the schematic diagram of all the designed fractures. The individual fracture design was adopted from numerous publications [27,29,35,42,46,52,62,71,77].

2.3.2. Core saturation

The typical saturation approach for conventional reservoir samples is ineffective for tight cores. Therefore, two saturation stages were performed to ensure the cores were fully saturated. Before conducting the saturation process, residual fluids inside the cores were removed by placing them in an oven at 248°F. Then the cores were left under a vacuum for two days to clean up the samples using a saturation vessel in stage A and two separate pumps, see Fig. 6. After vacuuming, each core is dry weighted as W_{dry}. The vessel was then filled with oil, after which the pump was resumed to begin the initial oil saturation procedure. The apparatus used for such processes involves a vacuum pump, a liquid trapper, and a saturation vessel. As soon as gas bubbles are absent from the vessel, the vacuum pump is turned off, and the cores are relocated to the high-pressure saturation vessel in stage B. The system in stage B mainly consists of an accumulator, a syringe pump, a pressure gauge, a stainless vessel, and an air bath oven. The syringe pump is used to reinject the oil into the vessel at high pressure through an accumulator. The accumulator has a piston that separates it into two sections: water and oil. In cooperation with the syringe pump, this piston pushes the oil slowly into the vessel that houses the core sample.

After the saturation pressure has reached 2100 psi, the pressure gauge is closely monitored. The pressure is maintained for seven days until no further pressure decrease is observed. To ensure that the pressure inside and outside the core reaches equilibrium and the degree of core saturation does not vary. Furthermore, the pressure is decreased very slowly while the temperature is maintained, as is the case in the oil field. However, a conventional saturation procedure was used to validate the modified saturation system. It is worth mentioning that the core temperature is maintained at a constant level throughout each complete test. When atmospheric pressure is reached, the saturated oil volume is measured. The calculated degree of saturation is then matched with the original porosity to confirm that the plugs are completely saturated. The weight of the core sample is then recorded as W_{sat}. At this point, the core is assumed to be 100% saturated and ready for the gas EOR injection processes.

2.3.3. Immiscible soaking procedure (first-step CO_2 soaking)

The procedures for the first CO_2 soaking are described in this section. The system was tested before the CO_2 injection by injecting N_2 at a pressure higher than the experimental pressure. First, the oil-saturated plug was placed inside the core holder according to the designed fracture shape (Fig. 2). Then, the backpressure was adjusted to a prespecified value to maintain a constant core pressure. Two backpressure regulators were included in the system. The CO_2 was then injected directly into the fracture until the pressure reached 800 psi. At that point, valve-1 was closed, and the core was aged for a soaking period. In this setup, only established channels are meant to represent fractures. Due to the high permeability contrast between the core matrix and fracture, CO_2 was mainly distributed through the fracture, enabling oil to be bypassed at various depths. The confining pressure was kept at 500 psi which was higher than the injection pressure to force the CO_2 to enter the fracture. After the soaking period, the backpressure was released through BPR-2. CO_2 was then injected at a constant flow rate of 25 ml/min for oil production using valve-2. By injecting CO_2 at a constant rate, the oil that came out to the surface during the soaking period was produced. Hence, the following miscible H-n-P process can be proficiently elucidated. The produced oil is accumulated, and its volume is measured. The procedures were continued until no additional oil was extracted. After one immiscible cycle is completed, the core sample was weighed (W_i) and the oil recovery was measured using Eq. (1). A series of such soaking procedures were performed using different fracture models and fracture dimensions. Some experiments were performed using fractured free and in-situ fractured core samples to obtain a clearer understanding and a conclusive conclusion.

$$\text{PercentOilRecoveryinImmiscibleSoakingCycle}i = \frac{wsat - wi}{wsat - wdry} \times 100 \qquad (1)$$

Note: W_{sat} is the weight of the core sample fully saturated with oil, W_i is the weight of the core sample after one soaking cycle, W_{dry} is the weight of the dry core sample.

2.3.4. Miscible CO_2 H-n-P procedure (second-step CO_2 soaking)

Following the abovementioned procedures, the CO_2 H-n-P experiment was performed utilizing the setups in Figs 3 and 4. The test was conducted after the first immiscible CO_2 soaking step aimed at extracting additional oil recovery and further simulating the FSA, similar to the H-n-P process in the depleted oil well. First, the CO_2 was injected into the accumulator to be stored at 800 psi. Then the pressure was increased to the desired level using the syringe pump. After injecting the CO_2 at 1750 psi into the fracture or the system, the inlet valve was closed, so the system began the second soaking stage. Subsequently, the puff stage was initiated; the system was put back into production mode by depressurizing the core holder to atmospheric pressure. Such pressurizing–soaking–depressurizing steps constitute a complete H-n-P cycle. After one completed cycle, the second one starts immediately, and so on. The same procedures were performed in the subsequent cycles. Each time, the weight of the core plug is documented, and oil recovery is

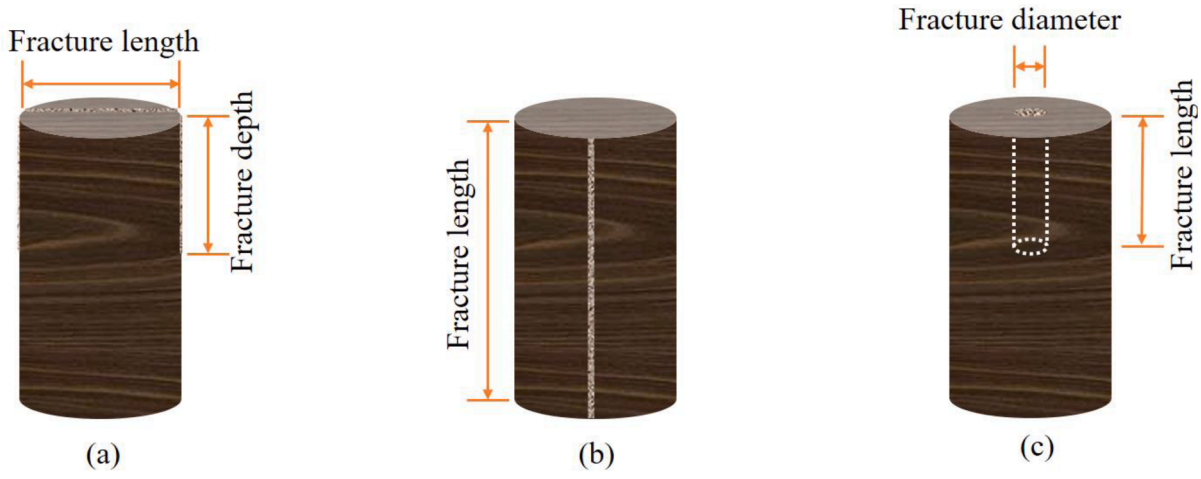

Fig. 5. Schematic of the designed artificial fractures.

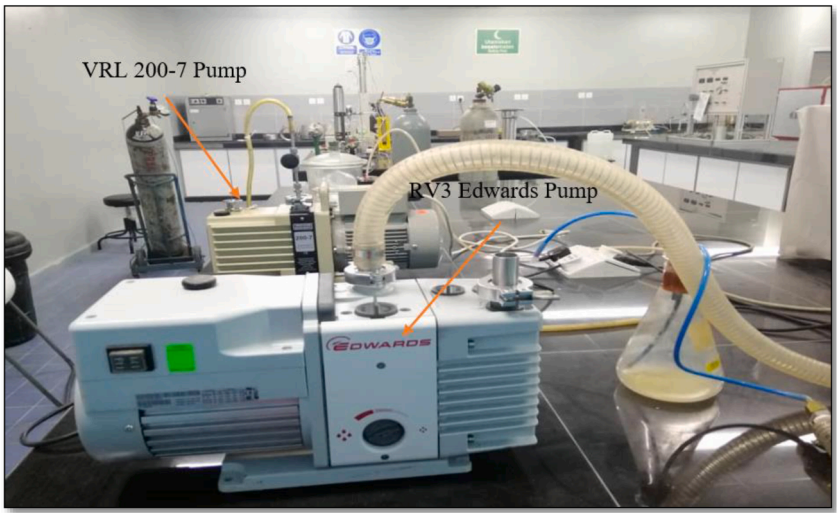

Fig. 6. Photograph of the vacuum pumps used to vacuum and saturate the core samples.

measured using Eq. (2). These CO_2 miscible cycles were repeated until no further obvious amounts of liquid oil was extracted.

$$\text{PercentOilRecoveryinMiscibleSoakingCycle}i = \frac{wsat - wi}{wsat - wdry} \times 100 \quad (2)$$

3. Results and discussion

3.1. Effect of the saturation system

When conducting a core flooding test, it is essential to measure the initial oil saturation of the core, so that the amount of oil extracted can be successfully measured. Incorrect saturation instruction can negatively affect the EOR experimental results. Generally, most literature on improving the saturation level mentions increasing the oil soaking times and soaking pressures [14]. However, only a few studies have reported the pressure depletion impact [75]; therefore, two different saturation scenarios were considered. The first case is that the pressure is gradually depleted after the oil-soaking process while the oven is kept on. The pressure is constantly lowered by 5 psi per hour to form a pressure depletion (PD). The core is weighed as soon as the soaking pressure reaches the atmospheric level. In the second scenario, the oven is turned off and the pressure is released in a short time (analogous to the conventional approach). Both processes are repeated using different core porosities. After each test is performed, the oil saturation porosity (φsat) is calculated and compared to the original gas porosity (φgas). The φgas is used as a reference value for porosity to compare it with the φsat results. Overall, φgas is moderately higher than φsat of fluid due to the low viscosity and small molecules. This allows the gas to flow easily into spaces of nano-pore size.

The results of core saturation indicate that, in the conventional scenario, an average of 90.83% of pore spaces are saturated with oil, while the percentage arrived at 97.41% in the low-pressure depletion methodology. The degree of oil saturation is equal to the ratio of saturated oil volume (oil-in-place) divided by the pore volume (PV) of the core and the value of the density of oil. The difference in weight between the weight of the dry core and the weight of the saturated core is the oil-in-place. The degree of oil saturation can be expressed by Eq. (3). Considering the obtained φsat for each group; it was observed that the low-pressure system had a greater influence on small pores media than the conventional structures. Even though the average oil saturation of both processes is above 90%, it is noteworthy that the improved degree of oil saturation is significant in evaluating the remaining oil extraction using soaking methodologies. The results of each applied method are very close, which implies that procedures were executed appropriately. The research findings revealed that higher pressure depletion time (PDT) triggers a higher level of saturation, especially in low porous media. As a result, rapid saturation pressure decline had a negative impact on saturation degree and made bypassed oil evaluation less efficient.

$$\text{DegreeofSaturation} = \frac{wsat - wi}{\rho oil - \text{p}\nu} \times 100 \quad (3)$$

3.2. Bypassed-oil recovery during immiscible CO_2 soaking

3.2.1. Effect of FSA on bypassed oil recovery using a confined system

Table 2 presents the fracture specifications of various investigated cores. All the experiments were executed under the same operating pressure; however, different fracture forms and surface areas were applied. In general, there is a frequent lack of clarification about the characteristics associated with hydraulic fractures. Thus, this section studies the significance of FW and FD, along with the fracture numbers. A conventional core holder with an overburden pressure system was used to efficiently assess the surface area's potential in oil recovery. Two artificial fracture types exhibited in Fig. 5, (a) and (b), were investigated. Both were constructed with a specially designed width and depth to emulate various FSAs. As a result of the confining pressure, the CO_2 was made to flow involuntarily along those dominant channels; therefore, only a limited area was affected by the injected CO_2. Only the oil wedged near the fracture was recovered efficiently. This is exactly the scenario of H-n-P performance in the oil field ([6]; Fiallos [25]). Based on the analysis of weight difference (see Table 3), the findings of the first pattern illustrate that the core with a greater fracture width has a lower recovery under the same operating conditions. The most critical factor in

Table 2
Fracture specifications and number of various investigated cores.

Sample	Status	Width, cm	Length, cm	Depth, cm	No of frac	Surface area per frac, cm^2
1	Fractured	0.2	4.9	1.3	1	13.72
2	Fractured	0.2	4.9	0.5	1	5.88
3	Fractured	0.5	4.9	2.6	1	27.93
4	Fractured	3	4.9	2	1	34.30
5	Fractured	0.5	4.9	3	1	31.85
6	Fractured	0.3	4	0.1	2	2.00
7	Fractured	0.3	4	0.1	4	2.00
8	Un-Fractured	/	/	/	/	/

Table 3
wt and total oil recovery after five cycles using various FSA.

Core weight, g	Cycle	Sample 3	Sample 4	Sample 5	Sample 6	Sample 7	Sample 8
Wi (initial), g	0	299.07	301.32	229.77	185.22	194.32	295.166
Wi, g	1	298.44	300.88	227.22	183.31	192.23	294.95
Wi, g	2	298.16	300.63	226.1	182.09	190.96	294.83
Wi, g	3	297.80	300.40	225.44	181.25	190.07	294.79
Wi, g	4	297.55	300.28	224.99	180.84	189.61	294.75
Wi, g	5	297.42	300.12	224.69	180.64	189.27	294.75
Total recovery,%		21.40	13.27	28.96	15.21	16.32	11.63

Note Wi: The weight of core sample after one cycle.

improving oil recovery is fracture depth because oil recovery increases dramatically in deeper fractures. In general, the results indicate that as the surface area of the fracture increases in-depth, the ratio of oil produced to oil in place also increases. However, the inverse scenario occurs when the fracture's surface area increases in width (Fig. 7). While the research demonstrates that a larger FSA results in increased oil recovery from deeper fractures, the significance of the surface area is unclear and unrelated to any particular trend. This may be attributed to the fracture model. Therefore, a different fracture shape is investigated in Section 3.4.3. The recovery from fractures with varying surface areas is depicted in Fig. 7. According to the observations, the intermediate FSA value of 31.85 cm^2 (Sample 5 in Table 1) has the highest recovery rate of 28%, while the highest FSA value of 34.30 cm^2 (Sample 4 in Table 1) has the lowest recovery rate of 13%. The above conclusion is consistent with that of Song et al. [64].

The results also demonstrate that the core with no fracture, FSA = 0 (sample 8 in Tables 1 and 2), had the lowest oil recovery (Fig. 7). Based on the results, it was established that to attain the desired economic oil volume, a deeper fracture requires less cycles. According to the results in Table 3, the intermediate FSA value of 31.85 cm^2 gives the highest recovery rate of 28%, whereas the highest FSA of 34.30 cm^2 gives nearly the lowest recovery rate of 13%. The recovery trend was reversed, with sample 2 generating less oil than sample 1, even though it had a smaller surface area (Fig. 8). Again, this is related to FD, not the total FSA. With a higher FD, a higher rate of oil recovery is achieved. This also confirms that the role of the FSA is unrelated to any trend. However, the results discussed herein can be used to improve the design of hydraulic fracturing operations, fluids, and additive packages used in tight oil reservoirs, and is expected to help decrease associated clean-up times and costs. In conclusion, deeper FSA yielded more oil. But, cracks having a narrow width and a great depth would maximize oil recovery.

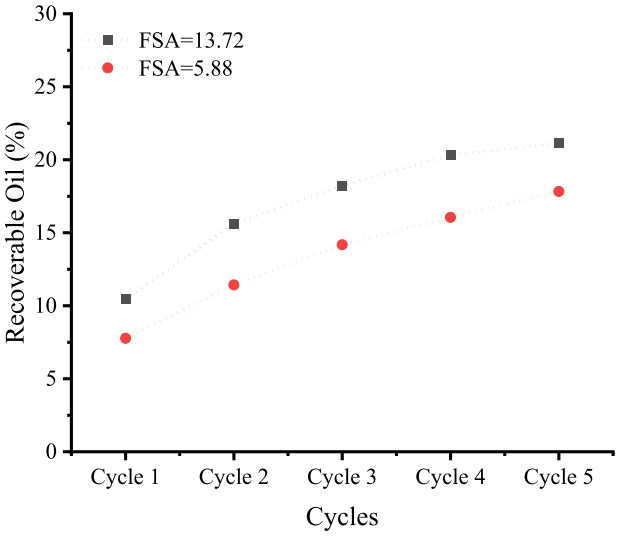

Fig. 8. Oil recovery from fractures that are the same in length and width but vary in depth.

An additional experiment was performed to validate the EOR efficiency using a more realistic reservoir condition. Specifically, a sandstone core with an in-situ fracture (Sample 9 in Table 1) was used in this test to get more accurate results. However, the FSA is unknown, indicating that FW and FD are undefined. The results shown in Fig. 9 demonstrate that both un-fractured and in-situ fractured cores had

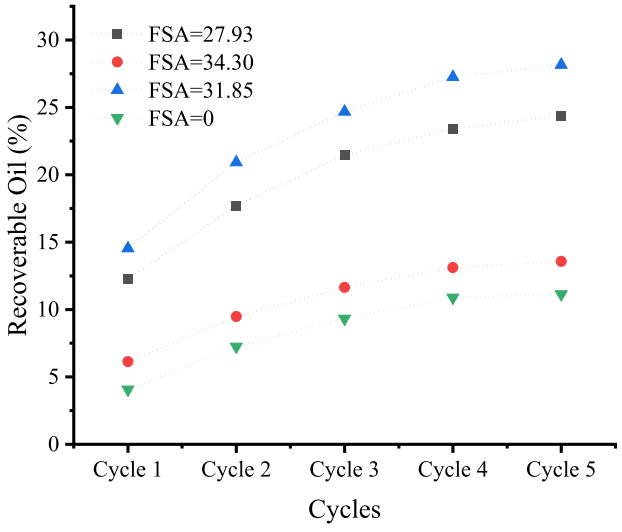

Fig. 7. The CO_2 soaking oil recovery per cycle under fracture and free fractured conditions.

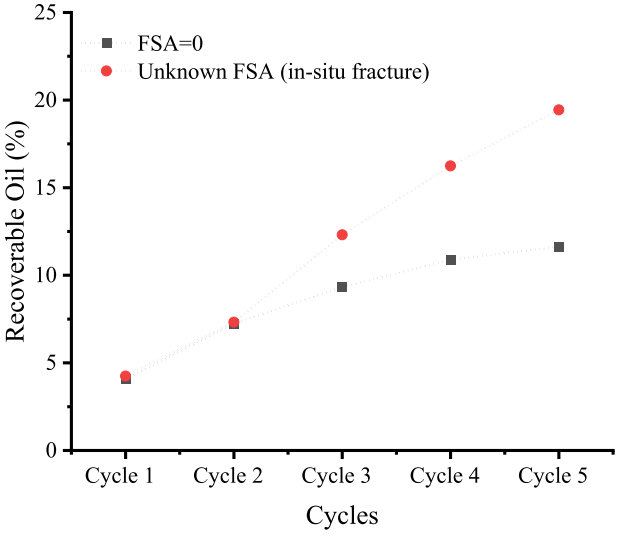

Fig. 9. The CO_2 soaking oil recovery from in-situ fractured core and other free fractured samples.

almost the same oil recovery during the first two cycles. Then sample 9's recovery increased significantly. After five cycles, Sample 9 delivered a 19% improvement in oil recovery, whereas Sample 8 produced only 11%. Therefore, the finding suggests that in situ FSA has little impact on oil recovery during the early soaking cycles. This may account for the CO_2 soaking process's poor performance in the low permeability oil field, despite promising laboratory results. Thus, it can be concluded that a confined core holder is a sufficient system for investigating the core FSAs. The discovery implies that in-situ FSA has little effect on oil recovery during the initial soaking cycles. The results also demonstrate the importance of utilizing EOR technology, particularly after well-completion operations are finished. Additionally, it emphasizes the critical use of an in-situ fracture model, especially in tight cores. Considering the particular pattern of fractures, an increase in fracture total (the number of fractures) results in a slight increase in oil recovery. For example, when the number of fractures per core is doubled from two to four, the total oil recovery increases by 0.62, as shown in Fig. 10. However, oil recovery increased by 1.65% during the first cycle, indicating that increasing the number of fractures significantly impacted the initial soaking cycles. This is consistent with the results recently reported by Mahzari et al. [46]. Although the number of fractures had a slightly significant effect on bypassed oil recovery using the confined system, the intensity of the fractures was thoroughly investigated.

3.2.2. *Effect of investigation system on bypassed oil recovery*

Similar investigative processes were performed using confined and unconfined core holders. Fig. 11 shows the recovery attained from two fracture-free cores, 10 and 11, using confined and unconfined systems, respectively. Contrary to confined system results, Sample 11 achieved the highest oil recovery using the unconfined core holder. The result is inconsistent with the conclusion earlier. The difference in oil recovery between the two modes reached 15%. This may be attributed to the investigative core holder, which plays a significant role in the CO_2 soaking recovery. Taking into account the individual pattern of fracture, less improvement in oil recovery occurs with an increase in fracture total. For instance, the oil recovery remains nearly constant when the fractures increase from 2 (Sample 12) to 4 (Sample 13) per core, as illustrated in Fig. 12. This indicates that artificial fractures have no effect since the system allows the gas to freely circulate all over the core by using the entire surface area of the plug, extracting oil from all sides. However, the most effective means to strip oil from tight cores with a permeability of less than 0.001 md is to use an unconfined system [14]. Once more, we acknowledge that using the free path core holder is not

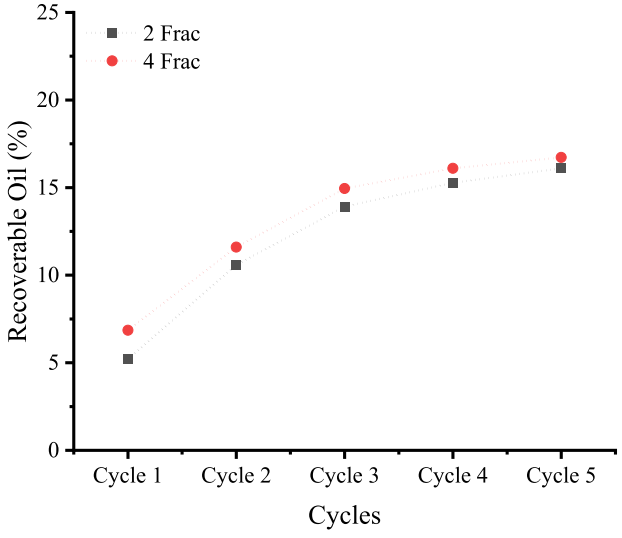

Fig. 10. Oil recovered was obtained from two fractures and four fractures per core using a confined system.

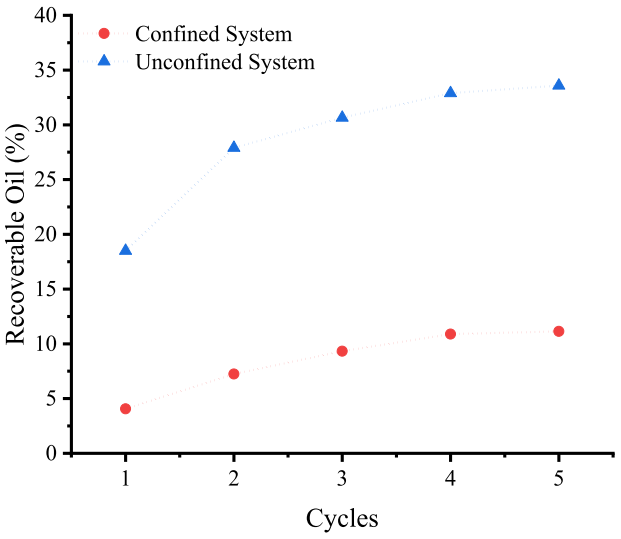

Fig. 11. The CO_2 soaking oil recovery per cycle for un-fractured core using confined and an unconfined pressure system.

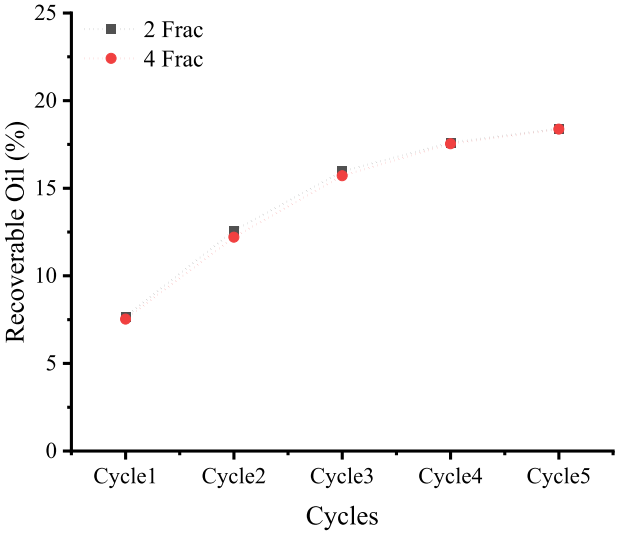

Fig. 12. Oil recovered was obtained from two fractures and four fractures per core using an unconfined system.

an accurate system to evaluate simulated cores. The results show that surface areas and fracture intensity are not as significant as they are in the confined system. Even though the average contact area between gas and oil has been enlarged, there is no evidential relationship between FSA and oil recovery. In general, the results indicate a major difference in the performance of CO_2 when different core holders are employed. The results obtained from an unconfined system may shed light on the substandard results of some lab tests despite the outstanding demonstration of competence of the simulation scale.

3.4. *Bypassed-oil recovery during CO_2 H-n-P, soaking step 2*

3.4.1. *Effect of miscible CO_2 soaking process on FSA using a confined system*

Following the immiscible protocols, the CO_2 H-n-P experiment was performed instantly to extract any remaining oil and further simulate the FSA. After completing the first-step soaking process for core Samples 1, 2, 3, 4, and 5, they were placed in the core holder shown in Fig. 3. Sensitivity experiments were conducted at a constant injection pressure

of 1750 psi. According to the findings in Fig. 13, CO_2 H-n-P has a significant effect on bypassed oil recovery, particularly in deep fractures. The highest oil recovery factors were observed in Samples 3 and 5. In Sample 5, approximately 54% of bypassed oil was effectively extracted. Although all cores demonstrated an increase in oil recovery, the increase was extremely modest in certain samples, such as Sample 4. Increased oil extraction occurs primarily as a result of CO_2's miscibility, which diffuses more easily into the deep fracture, reducing the viscosity and swelling of the oil. According to Adel et al. [4] and Tovar et al. [67], the dominant microscopic mechanisms are vaporization and oil expansion. Sun et al. [65] reported that incremental oil is sensitive to formation and fracture porosity, formation and fracture permeability, injection rate, cycling period, time of first injection, and the number of cycles. However, it is not sensitive to capillary pressure, diffusion coefficient, and length of soaking period. The results also indicate that when Fw is constant, the depth is the key factor. Although the volume of oil extracted using the two-step soaking methodology is less than previously reported results, this research confirms field pilot observations. This may demonstrate the relevance and importance of depleting fully saturated cores before initiating any H-n-P investigation. It's worth noting that both curves in Fig. 13 exhibit the same increasing trend, showing the higher level of certainty in determining FSA during immiscible and miscible processes.

3.4.2. *Effect of number of fractures on h-n-p recovery using a confined system*

The effect of the number of fractures on remaining oil recovery was also further investigated using Samples 6 and 7, with two and four fractures, respectively. To better understand the effect of fracture intensity, the recovery factor was calculated using data from eight cycles. All tests were conducted immediately after the first immiscible soaking process. Both samples demonstrated an increase in the recovery factor. As shown in Fig. 14, oil recovery from both samples increased significantly before declining. The RF of Sample 6 increased continuously until cycle 8. In contrast, owing to the close spacing of the fractures in Sample 7, oil recovery increased noticeably until cycle 5 and then remained constant, indicating that the number of cycles became less efficient. The conclusion was consistent with the results observed by Yu and Sheng [72], and Sie and Nguyen [59]. In terms of FSA, it has been demonstrated that samples with a larger surface area (more fractures) recover more initial recovery. FW and FD, on the other hand, are constant. This conclusion is consistent with that of Song et al. [62]. According to experimental findings, the number of H-n-P cycles is highly dependent on the number of formed fractures. As the number of fractures increases, the relative FSA increases, the relative matrix size decreases, and the apparent surface-to-volume ratio (AS/V) increases.

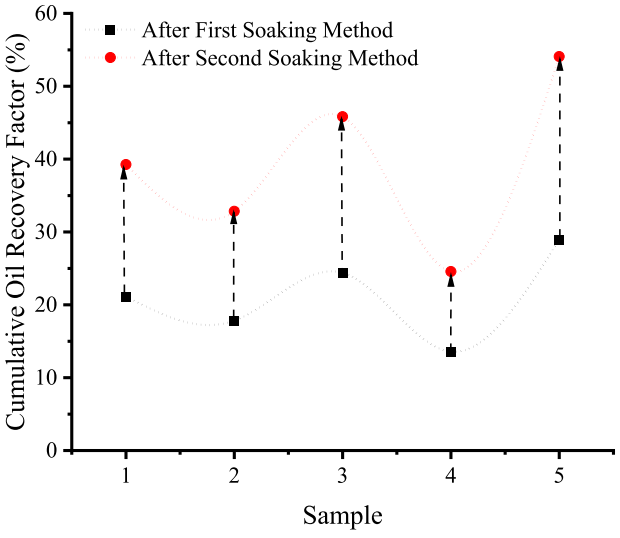

Fig. 13. Cumulative recovery factors from five cores with various FSAs during the miscible CO_2 H-n-P injection immediately following the immiscible process.

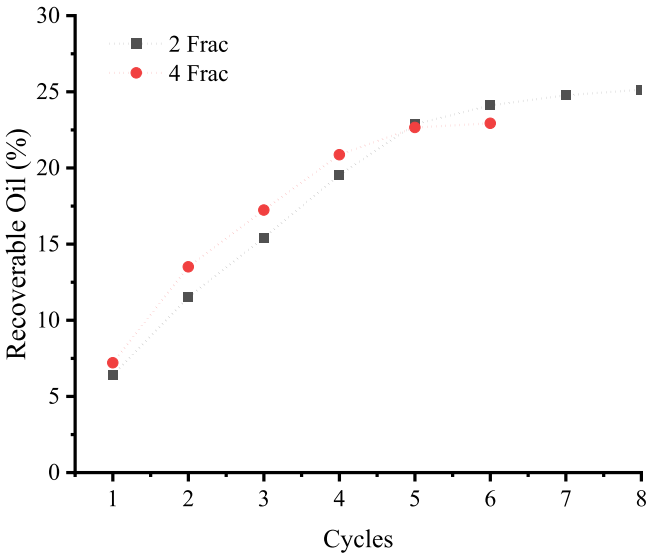

Fig. 14. The effect of the H-n-P cycle on oil recovery of two fractures and four fractures cores using a confined system.

The results confirm that oil recovery declines more rapidly in subsequent cycles than in initial cycles. Especially in the core with an increased fracture density. This is in line with the outcomes reported by Zhu et al. [77]. As shown in Fig. 14, the black and red lines intersect at a specific cycle, at which point the oil recovery rate begins to decline. Based on the dissection of both tested cores into sides and pieces, the CO_2 was found to spread more erratically and slowly in Sample 6, while in Sample 7, it spread faster towards the center of the core. This may be attributed to the number of applied fractures. CO_2 diffused slightly more slowly towards the center in a core with two fractures than in a core with four fractures, indicating that additional cycles are required to reach the economic rate. This may help to explain the continual increase in the RF in Sample 6 compared to Sample 7. Further research needs to be conducted using computer axial tomography (CAT) scanning and electrical resistivity (NMR) measurement to justify such observations better.

3.4.3. *Effect of FSA on bypassed oil recovery using hole fracture*

To precisely investigate the importance of FSA, three cores were drilled in the center at a depth of 3 cm and diameters of 0.2 cm, 0.3 cm, and 0.5 cm. The fractures had a surface area of 1.91 cm^2, 2.89 cm^2, and 4.90 cm^2, respectively. Such a matrix/core–fracture model has already been used to simulate shale oil by other investigators [35]. This study intended to systematically evaluate FSA's effect on CO_2 soaking potential using different fracture geometry or models (where gas can contact all sides of the fracture). The research can help in determining whether there are some zones with the optimum FSA for favorable oil recovery. After the CO_2 immiscible soaking process, the core was weighted and vertically placed in the confined core holder (Fig. 3). Miscible CO_2 was then injected into the fracture through valve-2, making contact with all core/matrix surfaces. As a result, the CO_2 traveled mostly along the designed hole fracture. The immiscible results demonstrate that fractures significantly impact oil recovery efficiency while increasing FSA in the matrix-fracture system improves the rate of oil recovery. Additionally, increasing FSA from 1.91 to 2.89 cm^2 only results in a 6.4% increase in RF, whereas increasing FSA from 2.89 to 4.90 cm^2 results in an 8.7% upsurge in recovery factor. The maximum recovery was achieved at the highest FSA condition with a value of 28.4% OOIP. A similar growth trend occurred during the miscible H-n-P process (Table 4). An increase of 23.2% OOIP of recovery factor was observed when the

Table 4
Summary of immiscible CO_2 process and CO_2 H-P results using different hole FSAs.

Test no.	FSA (cm^2)	RF, immiscible CO_2 soaking (%)	RF, CO_2 H-n-P (%)	RF, total (%)
1	1.91	13.3	36.5	49.8
2	2.89	19.7	33.2	52.9
3	4.90	28.4	30.7	59.1

reservoir condition was changed from immiscible to miscible using 1.91 cm^2 FSA. An increase in FSA, in general, adds a recovery factor. This is due to an increase in the average contact area between CO_2 and matrix oil, resulting in improved CO_2-oil interaction. Furthermore, the difference in total oil recovery achieved at various FSA conditions increased as the surface area of fracture increased. This implies that the higher the FSA, the more sensitive the oil RF is to it. This finding is consistent with the results of Min et al. [49].

While the recovery factor increased during the CO_2 immiscible soaking process, it decreased during the miscible CO_2 H-n-P activity, as illustrated in Fig. 15. In other words, as the FSA increases, the distance between the black and red lines narrows until they are nearly identical. This implies that FSA has a significant beneficial effect on oil recovery and the miscible CO_2 soaking process will eventually become less significant. This is because the immiscible process produced a large amount of oil, particularly at higher FSA values. This may demonstrate the effectiveness of the first-step soaking method before the H-n-P process. As shown in Fig. 15, increasing the surface area of the fracture significantly improves total oil recovery. These experiments demonstrate the vital nature of the surface area and the critical importance of comprehending the stimulated reservoir. This highlights the direct connection between the fracture geometry and the surface area of the stimulated reservoir.

4. Conclusions

1 Several significant new findings can be summarized as follows:
The performance of soaking process in fractured reservoirs is contingent upon the fracture geometry and thus on the FSA.
2 The most critical factor in optimizing oil recovery is fracture depth. While the research indicates that a larger FSA, results in increased oil recovery from a deeper fracture, the significance of the surface area is largely determined by the fracture design and investigation system.
3 Considering the number of fractures formed, an increase in fracture total results in a noticeable increase in oil recovery. However, such a conclusion is system-dependent.
4 The effectiveness of FSA depends on fracture geometry and pattern. This further highlighted the critical nature of fracture geometry concerning the surface area.
5 Due to the absence of field production data, this work concentrates on theoretical research that deviates from actual production. In the future, we plan to use numerical simulations in more in-depth research to demonstrate the importance of using realistic reservoir conditions and get a wider range of results that can help guide field production.

5. Recommendations

1 Internal mapping of the cores pre/post soaking would add value to our contribution. Therefore, further research utilizing CT or NMR measurements can provide valuable insights and better justify the research observations.

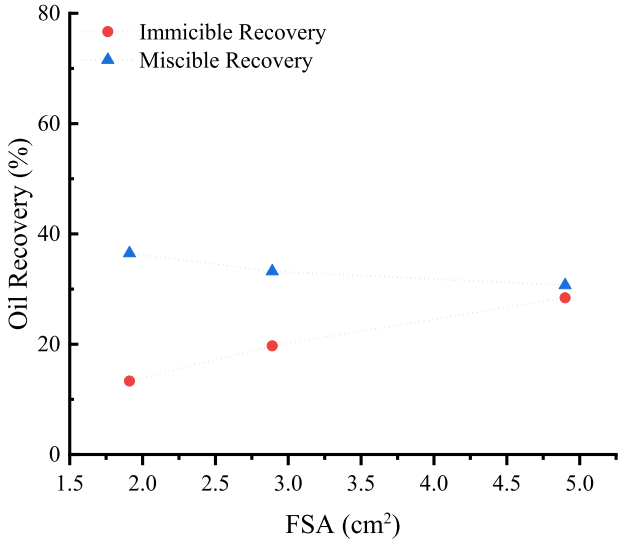

Fig. 15. Oil recovery vs. FSA during both miscible and immiscible CO_2 soaking process.

Declaration of Competing Interests

The authors declare that they have no known competing financial interests or personal relationships that could have appeared to influence the work reported in the submitted paper.

Acknowledgments

The authors would like to thank the Ministry of Higher Education and Scientific Research -Libya- for providing a scholarship. We are also grateful to Universiti Teknologi Malaysia for supporting this research through Research Management Grants Vot. No. R. J130000.3551.07G52, R.J130000.3551.06G68&06G69, R. J130000.2451.08G93, R.J 130000.3051.01M99, R.J 130000.7851.5F030 and R.J 130000.7351.4B545.

References

[1] H. Abdulelah, B.M. Negash, N. Yekeen, S. Al-Hajri, E. Padmanabhan, A. Al-Yaseri, Synergetic effect of surfactant concentration, salinity, and pressure on adsorbed methane in shale at low pressure: an experimental and modeling study, ACS Omega 5 (32) (2020) 20107–20121, https://doi.org/10.1021/acsomega.0c01738.
[2] P. Abolhosseini, M. Khosravi, B. Rostami, M. Masoudi, Influence of Thermal Marangoni convection on the recovery of bypassed oil during immiscible injection, J. Pet. Sci. Eng. 164 (2018) 196–205, https://doi.org/10.1016/j.petrol.2018.01.060.
[3] O. Adekunle, B.T. Hoffman, Experimental and analytical methods to determine minimum miscibility pressure (MMP) for Bakken formation crude oil, J. Pet. Sci. Eng. 146 (2016) 170–182, https://doi.org/10.1016/j.petrol.2016.04.013.
[4] I.A. Adel, F.D. Tovar, F. Zhang, D.S. Schechter, The impact of MMP on recovery factor during CO2 – EOR in unconventional liquid reservoirs, in: Proceedings of the SPE Annual Technical Conference and Exhibition, 2018.
[5] D. Alfarge, M. Wei, B. Bai, /03/01/). data analysis for CO2-EOR in shale-oil reservoirs based on a laboratory database, J. Pet. Sci. Eng. 162 (2018) 697–711, https://doi.org/10.1016/j.petrol.2017.10.087.
[6] D. Alfarge, M. Wei, B. Bai, Evaluating the performance of hydraulic-fractures in unconventional reservoirs using production data: comprehensive review, J. Nat. Gas Sci. Eng. 61 (2019) 133–141, https://doi.org/10.1016/j.jngse.2018.11.002.
[7] N. Alharthy, T. Teklu, H. Kazemi, R. Graves, S. Hawthorne, J. Braunberger, B. Kurtoglu, Enhanced oil recovery in liquid-rich shale reservoirs: laboratory to field, in: Proceedings of the SPE Annual Technical Conference and Exhibition, Houston, Texas, USA, 2015, https://doi.org/10.2118/175034-MS.
[8] F. Altawati, H. Emadi, R. Khalil, L. Heinze, H. Menouar, 2022/09/15/). an experimental investigation of improving wolfcamp shale-oil recovery using liquid-N2-assisted N2 and/or CO2 huff-n-puff injection technique, Fuel 324 (2022), 124450, https://doi.org/10.1016/j.fuel.2022.124450.
[9] W. Ampomah, R.S. Balch, M. Cather, R. Will, D. Gunda, Z. Dai, M.R. Soltanian, Optimum design of CO2 storage and oil recovery under geological uncertainty, Appl. Energy 195 (2017) 80–92, https://doi.org/10.1016/j.apenergy.2017.03.017.

[10] Y. Assef, P. Pereira Almao, Evaluation of cyclic gas injection in enhanced recovery from unconventional light oil reservoirs: effect of gas type and fracture spacing, Energies 12 (7) (2019) 1370. https://www.mdpi.com/1996-1073/12/7/1370.

[11] H. Bai, Q. Zhang, Z. Li, B. Li, D. Zhu, L. Zhang, G. Lv, Effect of fracture on production characteristics and oil distribution during CO2 huff-n-puff under tight and low-permeability conditions, Fuel 246 (2019) 117–125, https://doi.org/10.1016/j.fuel.2019.02.107.

[12] D.Z. Bejestani, B. Rostami, M. Khosravi, K. Kazemi, Effect of petrophysical matrix properties on bypassed oil recovery from a matrix-fracture system during CO2 near-miscible injection: experimental investigation, Int. J. Multiph. Flow 85 (2016) 123–131, https://doi.org/10.1016/j.ijmultiphaseflow.2016.06.011.

[13] C. Belu Mănescu, G. Nuño, /11/01/). Quantitative effects of the shale oil revolution, Energy Policy 86 (2015) 855–866, https://doi.org/10.1016/j.enpol.2015.05.015.

[14] L.C. Burrows, F. Haeri, P. Cvetic, S. Sanguinito, F. Shi, D. Tapriyal, A. Goodman, R. M. Enick, A literature review of CO2, natural gas, and water-based fluids for enhanced oil recovery in unconventional reservoirs, Energy Fuels 34 (5) (2020) 5331–5380, https://doi.org/10.1021/acs.energyfuels.9b03658.

[15] A.M. Bustin, R.M. Bustin, R. Downey, K. Venepalli, Laboratory analyses and compositional simulation of the eagle ford and wolfcamp shales: a novel shale oil EOR process, in: Proceedings of the SPE Improved Oil Recovery Conference, 2022.

[16] F. Castro-Alvarez, P. Marsters, D. Ponce de León Barido, D.M Kammen, Sustainability lessons from shale development in the United States for Mexico and other emerging unconventional oil and gas developers, Renew. Sustain. Energy Rev. 82 (2018) 1320–1332, https://doi.org/10.1016/j.rser.2017.08.082.

[17] L. Cheng, D. Wang, R. Cao, R. Xia, 2020/02/01/). The influence of hydraulic fractures on oil recovery by water flooding processes in tight oil reservoirs: an experimental and numerical approach, J. Pet. Sci. Eng. 185 (2020), 106572, https://doi.org/10.1016/j.petrol.2019.106572.

[18] A.J. Clark, Determination of recovery factor in the Bakken formation, Mountrail county, ND, in: Proceedings of the SPE Annual Technical Conference and Exhibition, 2009.

[19] S.E. Cudjoe, R. Barati Ghahfarokhi, R.H. Goldstein, J.S. Tsau, B. Nicoud, K. Bradford, A. Baldwin, D. Mohrbacher, An integrated workflow to characterize lower Eagle Ford shale for hydrocarbon gas huff-n-puff simulation, Fuel 289 (2021), 119854, https://doi.org/10.1016/j.fuel.2020.119854.

[20] S.E. Cudjoe, R. Barati, J.S. Tsau, C. Zhang, B. Nicoud, K. Bradford, A. Baldwin, D. Mohrbacher, Assessing the efficiency of saturating shale oil cores and evaluating hydrocarbon gas huff 'n' puff using nuclear magnetic resonance, SPE Reservoir Eval. Eng. (2021) 1–11, https://doi.org/10.2118/205027-pa.

[21] M. Ding, Y. Wang, Y. Wang, M. Gao, D. Liu, W. Chen, Experimental investigation of bypassed-oil recovery via CO2 soaking and huff and puff injection: effects of miscibility and bypassed-oil size, Fuel 248 (2019) 152–160, https://doi.org/10.1016/j.fuel.2019.03.088.

[22] D.-j. Du, W.-f. Pu, F.-y. Jin, R. Liu, Experimental study on EOR by CO2 huff-n-puff and CO2 flooding in tight conglomerate reservoirs with pore scale, Chem. Eng. Res. Des. 156 (2020) 425–432, https://doi.org/10.1016/j.cherd.2020.02.018.

[23] K. Elwegaa, H. Emadi, M. Soliman, T. Gamadi, M. Elsharafi, Improving oil recovery from shale oil reservoirs using cyclic cold carbon dioxide injection – an experimental study, Fuel 254 (2019), 115586, https://doi.org/10.1016/j.fuel.2019.05.169.

[24] S. Fakher, A. Imqam, Application of carbon dioxide injection in shale oil reservoirs for increasing oil recovery and carbon dioxide storage, Fuel 265 (2020), 116944, https://doi.org/10.1016/j.fuel.2019.116944.

[25] M.X. Fiallos Torres, W. Yu, R. Ganjdanesh, E. Kerr, K. Sepehrnoori, J. Miao, R Ambrose, Modeling interwell fracture interference and huff-n-puff pressure containment in eagle ford using EDFM, in: Proceedings of the SPE Oklahoma City Oil and Gas Symposium, 2019.

[26] T.D. Gamadi, J.J. Sheng, M.Y. Soliman, H. Menouar, M.C. Watson, H. Emadibaladehi, An experimental study of cyclic CO2 injection to improve shale oil recovery, in: Proceedings of the SPE Improved Oil Recovery Symposium, Tulsa, Oklahoma, USA, 2014, https://doi.org/10.2118/169142-MS.

[27] A. Ghanizadeh, C. Song, H. Hamdi, C.R. Clarkson, Experimental and computational evaluation of cyclic solvent injection in fractured tight hydrocarbon reservoirs, Sci. Rep. 11 (1) (2021) 9497, https://doi.org/10.1038/s41598-021-88247-y.

[28] X. Gong, R. Gonzalez, D.A. McVay, J.D. Hart, Bayesian probabilistic decline-curve analysis reliably quantifies uncertainty in shale-well-production forecasts, SPE J. 19 (06) (2014) 1047–1057, https://doi.org/10.2118/147588-pa.

[29] S. Goyal, M.E. Curtis, C.H. Sondergeld, C.S. Rai, A Comparative study of monotonic and cyclic injection hydraulic fracturing in saturated tight rocks under triaxial stress, in: Proceedings of the SPE/AAPG/SEG Unconventional Resources Technology Conference, 2020.

[30] M. Hao, S. Liao, G. Yu, X. Lei, Y. Tang, Performance optimization of CO_2huff-n-puff for multifractured horizontal wells in tight oil reservoirs, Geofluids 2020 (2020), 8840384, https://doi.org/10.1155/2020/8840384.

[31] J. Ivory, J. Chang, R. Coates, K. Forshner, Investigation of cyclic solvent injection process for heavy oil recovery, J. Can. Pet. Technol. 49 (09) (2010) 22–33, https://doi.org/10.2118/140662-pa.

[32] R.B. Jackson, A. Vengosh, J.W. Carey, R.J. Davies, T.H. Darrah, F. O'Sullivan, G. Pétron, The environmental costs and benefits of fracking, Annu. Rev. Environ. Resour. 39 (1) (2014) 327–362, https://doi.org/10.1146/annurev-environ-031113-144051.

[33] T. Jacobs, Shale EOR delivers, so why won't the sector go big? J. Pet. Technol. 71 (05) (2019) 37–41, https://doi.org/10.2118/0519-0037-jpt.

[34] X. Jia, F. Zeng, Y. Gu, Gasflooding-assisted cyclic solvent injection (GA-CSI) for enhancing heavy oil recovery, Fuel 140 (2015) 344–353, https://doi.org/10.1016/j.fuel.2014.09.066.

[35] Y. Jia, Y. Lu, D. Elsworth, Y. Fang, J. Tang, Surface characteristics and permeability enhancement of shale fractures due to water and supercritical carbon dioxide fracturing, J. Pet. Sci. Eng. 165 (2018) 284–297, https://doi.org/10.1016/j.petrol.2018.02.018.

[36] L. Jin, S. Hawthorne, J. Sorensen, L. Pekot, B. Kurz, S. Smith, L. Heebink, V. Herdegen, N. Bosshart, J. Torres, C. Dalkhaa, K. Peterson, C. Gorecki, E. Steadman, J. Harju, Advancing CO2 enhanced oil recovery and storage in unconventional oil play—Experimental studies on Bakken shales, Appl. Energy 208 (2017) 171–183, https://doi.org/10.1016/j.apenergy.2017.10.054.

[37] K. Joslin, A.M. Abraham, T. Thaker, V. Pathak, A. Kumar, Viability of EOR processes in the Bakken under geological and economic uncertainty, in: Proceedings of the SPE Canada Unconventional Resources Conference, 2018.

[38] B. Li, H. Bai, A. Li, L. Zhang, Q. Zhang, Experimental investigation on influencing factors of CO2 huff and puff under fractured low-permeability conditions, Energy Sci. Eng. 7 (5) (2019) 1621–1631, https://doi.org/10.1002/ese3.376.

[39] L. Li, J.J. Sheng, Y. Su, S. Zhan, Further investigation of effects of injection pressure and imbibition water on CO2 huff-n-puff performance in liquid-rich shale reservoirs, Energy Fuels 32 (5) (2018) 5789–5798, https://doi.org/10.1021/acs.energyfuels.8b00536.

[40] L. Li, C. Wang, D. Li, J. Fu, Y. Su, Y. Lv, Experimental investigation of shale oil recovery from Qianjiang core samples by the CO2 huff-n-puff EOR method [10.1039/C9RA05347F], RSC Adv. 9 (49) (2019) 28857–28869, https://doi.org/10.1039/C9RA05347F.

[41] L. Li, Y. Zhang, J.J. Sheng, Effect of the injection pressure on enhancing oil recovery in shale cores during the CO2 huff-n-puff process when it is above and below the minimum miscibility pressure, Energy Fuels 31 (4) (2017) 3856–3867, https://doi.org/10.1021/acs.energyfuels.7b00031.

[42] X. Li, Z. Feng, G. Han, D. Elsworth, C. Marone, D. Saffer, Hydraulic fracturing in shale with H2O, CO2 and N2, in: Proceedings of the 49th U.S. Rock Mechanics/Geomechanics Symposium, 2015.

[43] Z. Li, Y. Gu, Soaking effect on miscible CO2 flooding in a tight sandstone formation, Fuel 134 (2014) 659–668, https://doi.org/10.1016/j.fuel.2014.06.024.

[44] S. Liu, V. Sahni, J. Tan, D. Beckett, T. Vo, Laboratory investigation of EOR techniques for organic rich shales in the permian basin, in: Proceedings of the SPE/AAPG/SEG Unconventional Resources Technology Conference, 2018.

[45] P. Mahzari, A.P. Jones, E.H. Oelkers, An integrated evaluation of enhanced oil recovery and geochemical processes for carbonated water injection in carbonate rocks, J. Pet. Sci. Eng. 181 (2019), 106188, https://doi.org/10.1016/j.petrol.2019.106188.

[46] P. Mahzari, T.M. Mitchell, A.P. Jones, E.H. Oelkers, A. Striolo, F. Iacoviello, P. R. Shearing, J. Ernesto Juri, 2021/01/15/). Novel laboratory investigation of huff-n-puff gas injection for shale oils under realistic reservoir conditions, Fuel 284 (2021), 118950, https://doi.org/10.1016/j.fuel.2020.118950.

[47] S. Malo*, J. McNamara, N. Volkmer, E Amirian, Eagle ford ? introducing the big bad wolf, in: Proceedings of the Unconventional Resources Technology Conference (URTeC); Society of Exploration Geophysicists, 2019, pp. 4733–4743, https://doi.org/10.15530/urtec-2019-624, 10.15530/urtec-2019-624.

[48] M. Milad, R. Junin, A. Sidek, A. Imqam, M. Tarhuni, Huff-n-Puff technology for enhanced oil recovery in shale/tight oil reservoirs: progress, gaps, and perspectives, Energy Fuels (2021), https://doi.org/10.1021/acs.energyfuels.1c02561.

[49] B. Min, S. Mamoudou, S. Dang, A. Tinni, C. Sondergeld, C. Rai, Comprehensive experimental study of huff-n-puff enhanced oil recovey in eagle ford: key parameters and recovery mechanism, in: Proceedings of the SPE Improved Oil Recovery Conference, 2020.

[50] G. Niu, D. Schechter, Insights into field application of EOR techniques from modeling of tight reservoirs with complex high-density fracture network, in: Proceedings of the SPE Improved Oil Recovery Conference, 2020.

[51] W. Ozowe, S. Zheng, M. Sharma, 2020/12/01/). Selection of hydrocarbon gas for huff-n-puff IOR in shale oil reservoirs, J. Pet. Sci. Eng. 195 (2020), 107683, https://doi.org/10.1016/j.petrol.2020.107683.

[52] M. Parvazdavani, S. Abbasi, M. Zare-Reisabadi, Experimental study of gas–oil relative permeability curves at immiscible/near miscible gas injection in highly naturally fractured reservoir, Egypt. J. Pet. 26 (1) (2017) 171–180, https://doi.org/10.1016/j.ejpe.2016.01.002.

[53] W.F. Pu, D.J. Du, S. Wang, L. Zeng, R. Feng, S. Memon, J. Sarout, M. A. Varfolomeev, M. Sarmadivaleh, Q. Xie, Experimental study of CO2 huff-n-puff in a tight conglomerate reservoir using true triaxial stress cell core fracturing and displacement system: a case study, J. Pet. Sci. Eng. 199 (2021), 108298, https://doi.org/10.1016/j.petrol.2020.108298.

[54] K. Qian, S. Yang, H. Dou, Q. Wang, L. Wang, Y. Huang, Experimental investigation on microscopic residual oil distribution during CO2 huff-and-puff process in tight oil reservoirs, Energies 11 (10) (2018) 2843. https://www.mdpi.com/1996-1073/11/10/2843.

[55] J.F. Ramirez, R. Aguilera, Factors controlling fluid migration and distribution in the eagle ford shale, SPE Reservoir Eval. Eng. 19 (03) (2016) 403–414, https://doi.org/10.2118/171626-pa.

[56] J.J. Sheng, Optimization of huff-n-puff gas injection in shale oil reservoirs, Petroleum 3 (4) (2017) 431–437, https://doi.org/10.1016/j.petlm.2017.03.004.

[57] J.J. Sheng, J.J. Sheng, Chapter Two - Huff-n-puff gas injection in oil reservoirs. Enhanced Oil Recovery in Shale and Tight Reservoirs, Gulf Professional Publishing, 2020, pp. 7–60, https://doi.org/10.1016/B978-0-12-815905-7.00002-5.

[58] J.J. Sheng, K. Chen, Evaluation of the EOR potential of gas and water injection in shale oil reservoirs, J. Unconv. Oil Gas Resour. 5 (2014) 1–9, https://doi.org/10.1016/j.juogr.2013.12.001.
[59] C.Y. Sie, Q.P. Nguyen, Laboratory investigations on field gas huff-n-puff for improving oil recovery in eagle ford shale–effect of operating conditions, Energy Fuels (2021), https://doi.org/10.1021/acs.energyfuels.1c03003.
[60] D.J. Soeder, The successful development of gas and oil resources from shales in North America, J. Pet. Sci. Eng. 163 (2018) 399–420, https://doi.org/10.1016/j.petrol.2017.12.084.
[61] C. Song, C.R. Clarkson, H. Hamdi, A. Ghanizadeh, Evaluation of cyclic solvent injection (?huff-n-puff˙) in artificially-fractured shale core samples: experiments & modeling, in: Proceedings of the Unconventional Resources Technology Conference, Virtual, 20?22 July 2020 (pp. 2794-2813). Unconventional Resources Technology Conference (URTeC), 2020, https://doi.org/10.15530/urtec-2020-3038, 10.15530/urtec-2020-3038.
[62] C. Song, C.R. Clarkson, H. Hamdi, A. Ghanizadeh, Evaluation of cyclic solvent injection ('Huff-n-Puff, in: Proceedings of the Artificially-Fractured Shale Core Samples: Experiments & Modeling. SPE/AAPG/SEG Unconventional Resources Technology Conference, 2020.
[63] Z. Song, J. Hou, X. Liu, Q. Wei, H. Hao, L. Zhang, Conformance control for CO2-EOR in naturally fractured low permeability oil reservoirs, J. Pet. Sci. Eng. 166 (2018) 225–234, https://doi.org/10.1016/j.petrol.2018.03.030.
[64] Z. Song, Y. Li, Y. Song, B. Bai, J. Hou, K. Song, A. Jiang, S. Su, A critical review of CO2 enhanced oil recovery in tight oil reservoirs of North America and China, in: Proceedings of the SPE/IATMI Asia Pacific Oil & Gas Conference and Exhibition, 2019.
[65] J. Sun, A. Zou, E. Sotelo, D. Schechter, Numerical simulation of CO2 huff-n-puff in complex fracture networks of unconventional liquid reservoirs, J. Nat. Gas Sci. Eng. 31 (2016) 481–492, https://doi.org/10.1016/j.jngse.2016.03.032.
[66] W. Tang, J.J. Sheng, Huff-n-puff gas injection or gas flooding in tight oil reservoirs? J. Pet. Sci. Eng. 208 (2022), 109725 https://doi.org/10.1016/j.petrol.2021.109725.
[67] F.D. Tovar, M.A. Barrufet, D.S. Schechter, Gas Injection for EOR in organic rich shale. part I: operational philosophy, in: Proceedings of the SPE Improved Oil Recovery Conference, 2018.
[68] S. Wu, Z. Li, Z. Wang, H.K. Sarma, C. Zhang, M. Wu, Investigation of CO2/N2 injection in tight oil reservoirs with confinement effect, Energy Sci. Eng. 8 (4) (2020) 1194–1208, https://doi.org/10.1002/ese3.578.
[69] X. Xiong, J.J. Sheng, X. Wu, J. Qin, Experimental investigation of foam-assisted N2 huff-n-puff enhanced oil recovery in fractured shale cores, Fuel 311 (2022), 122597, https://doi.org/10.1016/j.fuel.2021.122597.
[70] W. Xue-wu, X. Pufu, Y. Zheng-ming, L. Xue-wei, X. Zhi-zeng, W. Li-qiang, Laboratory and field-scale parameter optimization of CO2 huff–n–puff with the staged-fracturing horizontal well in tight oil reservoirs, J. Pet. Sci. Eng. 186 (2020), 106703, https://doi.org/10.1016/j.petrol.2019.106703.
[71] Z. Ye, M. Janis, A. Ghassemi, S. Riley, Laboratory investigation of fluid flow and permeability evolution through shale fractures, in: Proceedings of the SPE/AAPG/SEG Unconventional Resources Technology Conference, 2017.
[72] Y. Yu, J.J. Sheng, An experimental investigation of the effect of pressure depletion rate on oil recovery from shale cores by cyclic N2 injection, in: Proceedings of the SPE/AAPG/SEG Unconventional Resources Technology Conference, 2015.
[73] T. Zeng, C. Miller, K.K. Mohanty, Use of gas and chemical blend for shale oil huff-n-puff EOR, in: Proceedings of the SPE/AAPG/SEG Unconventional Resources Technology Conference, 2020.
[74] F. Zhang, D.S. Schechter, Gas and foam injection with CO2 and enriched NGL's for enhanced oil recovery in unconventional liquid reservoirs, J. Pet. Sci. Eng. 202 (2021), 108472, https://doi.org/10.1016/j.petrol.2021.108472.
[75] T. Zheng, Z. Yang, X. Liu, Y. Luo, Q. Xiao, Y. Zhang, X. Zhao, Understanding immiscible natural gas huff-n-puff seepage mechanism in porous media: a case study of CH4 huff-n-puff by laboratory numerical simulations in chang-7 tight core, Nat. Resour. Res. 30 (3) (2021) 2397–2411, https://doi.org/10.1007/s11053-021-09836-2.
[76] C.F. Zhu, W. Guo, Y.P. Wang, Y.J. Li, H.J. Gong, L. Xu, M.Z. Dong, Experimental study of enhanced oil recovery by CO2 huff-n-puff in shales and tight sandstones with fractures, Pet. Sci. (2020), https://doi.org/10.1007/s12182-020-00538-7.
[77] C.F. Zhu, W. Guo, Y.P. Wang, Y.J. Li, H.J. Gong, L. Xu, M.Z. Dong, Experimental study of enhanced oil recovery by CO2 huff-n-puff in shales and tight sandstones with fractures, Pet. Sci. 18 (3) (2021) 852–869, https://doi.org/10.1007/s12182-020-00538-7.